

Supramolecular Squares with Mo₂⁴⁺ CornersF. Albert Cotton,^{*,†} Chun Lin,[†] and Carlos A. Murillo^{*,†,‡}

Department of Chemistry and Laboratory for Molecular Structure and Bonding, P.O. Box 300012, Texas A&M University, College Station, Texas 77842-3012 and Department of Chemistry, University of Costa Rica, Ciudad Universitaria, Costa Rica

Received September 7, 2000

Seven complexes obtained by reacting the quadruply bonded complex [Mo₂(*cis*-DAniF)₂(CH₃CN)₄](BF₄)₂ (DAniF = *N,N'*-di-*p*-anisylformamidinate) and (Buⁿ₄N⁺)₂(Carb²⁻), where Carb²⁻ is a dicarboxylate anion, have been found to have a ratio of dimetal unit to dicarboxylate of 1:1. As noted by the carboxylate linker, the compounds are oxalate, **1**, fumarate, **2**, ferrocene dicarboxylate, **3**, 4,4'-biphenyldicarboxylate, **4**, acetylenedicarboxylate, **5**, tetrafluorophthalate, **6**, and carborane dicarboxylate, **7**. Structural characterization of **1–4** revealed a square of dimolybdenum units linked by the dicarboxylate anions, each having an interstice capable of accommodating specific solvent molecules. Results of NMR studies of all seven compounds are consistent with the presence of a highly symmetrical structure. These compounds display a rich electrochemical behavior that is affected by the nature of the carboxylate group.

Introduction

The use of metal atoms (or ions) as key elements in the assembly of supramolecular arrays has emerged as an area of great—and still increasing—interest over the past few years.¹ It has been pointed out that with proper choice of metal-containing units, a great variety of polygons and polyhedra should be obtainable; some of them have already been realized, but often X-ray structures of the larger ones have been lacking. In most of the work done in other laboratories, the metal-containing moiety has been a *cis*-ML₂ (M = Pd^{II}, Pt^{II}) unit, where the L ligands (or bidentate L₂ ligand) are neutral. Since the linkers, usually diamines, are also neutral, the polygons or polyhedra containing *n* metal moieties have charges of 2*n*⁺, usually upward of 8⁺. Only in a very few cases has a neutral metal moiety, e.g., Re(CO)₃Cl,² been used together with neutral linkers, thus leading to a neutral product. In these compounds, no change in the charge is in general possible because oxidation or reduction would lead to disintegration of the assembly.

We have chosen to pursue a quite different approach to synthesizing supramolecular arrays based on the use of metal atoms to dictate overall molecular geometry, namely, the use

of dimetal units (Mo₂⁴⁺, Rh₂⁴⁺, etc.) that are partly encumbered by nonlabile ligands. Examples are shown in Scheme 1. These metal–metal bound units, which bear some positive charge, are then combined with linkers that are anionic, typically (but not necessarily) the anions of dicarboxylic acids, so that the supramolecular products so obtained are neutral molecules.

The dimetal units, when combined with the appropriate linkers, are capable of producing as great a variety of structures as the mononuclear metal moieties but with the added advantage that the products are amenable to redox chemistry. Scheme 2 shows some of the more obvious one- and two-dimensional possibilities, some of which have already been reported in preliminary form.^{3,4} A three-dimensional product has also been the subject of a preliminary report.⁵

This paper is the second of a series of reports in which the full details of our work will be presented. We are concerned here with seven compounds, four (and possibly all) of which are molecular squares based on Mo₂⁴⁺ corner pieces. Scheme 3 shows the general square structure and the seven dicarboxylate linkers.

Experimental Section

General Considerations. All the syntheses were performed under a dry nitrogen atmosphere using standard Schlenk techniques. Solvents were dried, then distilled under nitrogen following conventional methods. Chemicals were purchased from Aldrich and used as received. The tetrabutylammonium salts were prepared by neutralizing the corresponding dicarboxylic acid with 1.0 M Buⁿ₄NOH in MeOH solution, followed by vacuum-drying at 40–50 °C for 24 h. The compound Mo₂(*cis*-DAniF)₂(CH₃CN)₄(BF₄)₂ (DAniF = *N,N'*-di-*p*-anisylformamidinate) was prepared by following published procedures.⁶

* To whom correspondence should be addressed. E-mail: cotton@tamu.edu or murillo@tamu.edu.

† Texas A&M University.

‡ University of Costa Rica.

- (1) (a) Leininger, S.; Olenyuk, B.; Stang, P. J. *Chem. Rev.* **2000**, *100*, 853 and references therein. (b) Fujita, M. *Chem. Soc. Rev.* **1998**, *27*, 417 and references therein. (c) Espinet, P.; Soulantica, K.; Charmant, J. P. H.; Orpen, A. G. *Chem. Commun.* **2000**, 915. (d) Navarro, J. A. R.; Lippert, B. *Coord. Chem. Rev.* **1999**, *185–186*, 653. (e) Whang, D.; Kim, K. *J. Am. Chem. Soc.* **1997**, *119*, 451. (f) Mann, S.; Huttner, G.; Zsolnai, Li; Heinze, K. *Angew. Chem., Int. Ed. Engl.* **1996**, *35*, 2808. (g) Scherer, M.; Caulder, D. L.; Johnson, D. W.; Raymond, K. N. *Angew. Chem., Int. Ed. Engl.* **1999**, *38*, 1588. (h) Benkstein, K. D.; Hupp, J. T.; Stern, C. L. *Inorg. Chem.* **1998**, *37*, 5404. (i) Lai, S.-W.; Chan, M. C.-W.; Peng, S.-M.; Che, C.-M. *Angew. Chem., Int. Ed. Engl.* **1999**, *38*, 669. (j) Jones, C. J. *Chem. Soc. Rev.* **1998**, *27*, 289. (k) Klausmeyer, K. K.; Wilson, S. R.; Rauchfuss, T. B. *J. Am. Chem. Soc.* **1999**, *121*, 2705.
- (2) Stone, R. V.; Hupp, J. T.; Albrecht-Schmitt, T. E. *Inorg. Chem.* **1996**, *35*, 4096.

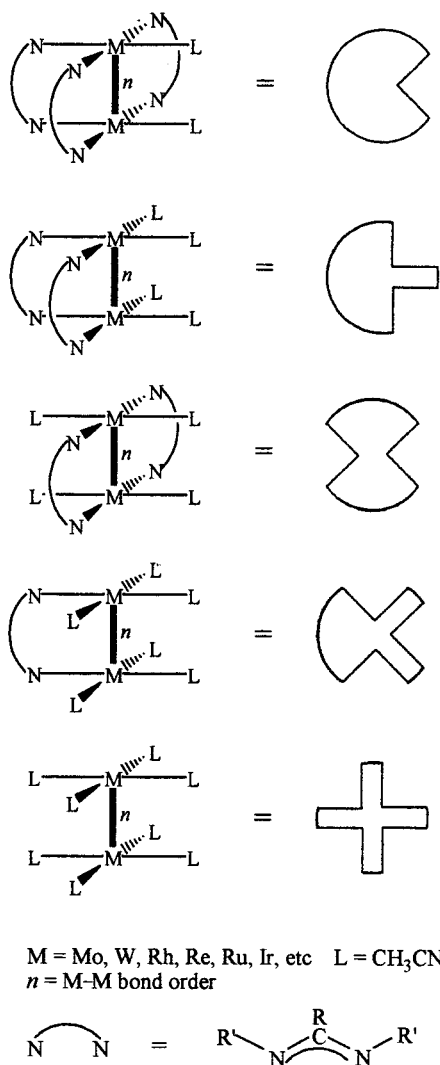
(3) Cotton, F. A.; Daniels, L. M.; Lin, C.; Murillo, C. A. *J. Am. Chem. Soc.* **1999**, *121*, 4538.

(4) Cotton, F. A.; Lin, C.; Murillo, C. A. *J. Chem. Soc., Dalton Trans.* **1998**, 3151.

(5) Cotton, F. A.; Daniels, L. M.; Lin, C.; Murillo, C. A. *Chem. Commun.* **1999**, 841.

(6) Chisholm, M. H.; Cotton, F. A.; Daniels, L. M.; Folting, K.; Huffman, J.; Iyer, S.; Lin, C.; Macintosh, A. M.; Murillo, C. A. *J. Chem. Soc., Dalton Trans.* **1999**, 1387.

Scheme 1

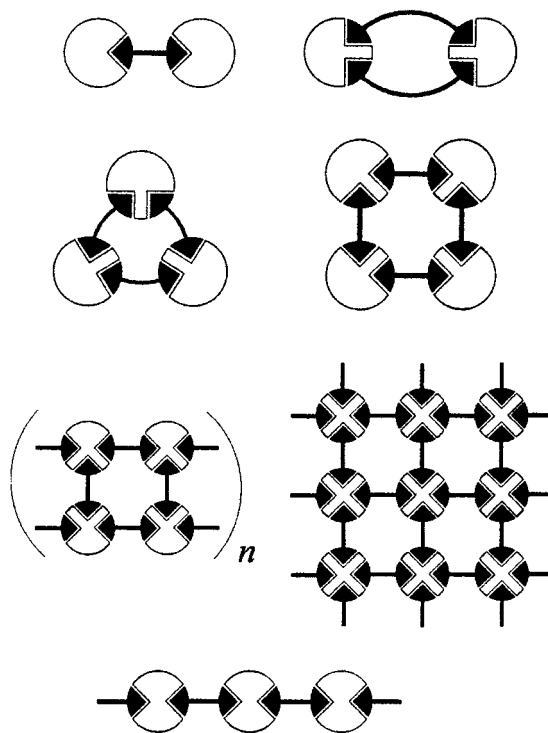


Elemental analyses were performed by Canadian Microanalytical Service, Delta, British Columbia; the results were satisfactory. The cyclic voltammograms were recorded on a BAS 100 electrochemical analyzer in 0.10 M Bu₄NPF₆ solution (CH₂Cl₂) with Pt working and auxiliary electrodes, a Ag/AgCl reference electrode, and scan rates of 100 mV s⁻¹. All the potential values are referenced to the Ag/AgCl electrode, and under the present experimental conditions, the E_{1/2}(Fc⁺/Fc) was consistently measured to be 440 mV.

Preparation of Complexes. [*cis*-Mo₂(DAniF)₂]₄(O₂CCO₂)₄ (**1**). A similar preparation method was used for compounds **2–7**. To a stirred solution of [Mo₂(*cis*-DAniF)₂(CH₃CN)₄][BF₄]₂ (312 mg, 0.300 mmol) in 30 mL of CH₃CN was added [Bu₄N]₂[C₂O₄] (180 mg, 0.310 mmol) in 20 mL of CH₃CN. An immediate reaction took place with the formation of a bright-red precipitate, which was collected by filtration, washed several times with CH₃CN, and dried under vacuum. The crude product was extracted with CH₂Cl₂ (3 × 5 mL). Hexanes were then carefully layered on the top of the solution to afford a bright-red crystalline material after 7 days. Yield: 205 mg, 86% (after elimination of the interstitial molecules). Anal. Calcd (found) for **1**, C₁₂₈H₁₂₀-Mo₈N₁₆O₃₂: C, 48.62 (48.27); H, 3.83 (3.88); N, 7.09 (7.10). ¹H NMR δ (ppm, in CD₂Cl₂): 8.57 (s, 8H, CNCHNC), 6.65 (dd, 64H, aromatic), 3.70 (s, 48H, -OCH₃).

[*cis*-Mo₂(DAniF)₂]₄(*trans*-O₂CCH=CHCO₂)₄ (**2**). Crude product was recrystallized from CH₂Cl₂/hexanes solution. The product was dark-red. Yield: 230 mg, 94%. Anal. Calcd (found) for **2**, C₁₃₆H₁₂₈-Mo₈N₁₆O₃₂: C, 50.01 (49.45); H, 3.95 (3.96); N, 6.86 (6.63). Single crystals suitable for X-ray analysis were grown by diffusion of toluene into a CH₂Cl₂ solution. ¹H NMR δ (ppm, in CD₂Cl₂): 8.51 (s, 8H,

Scheme 2



-NCHN-), 7.36 (s, 8H, -HC=CH-), 6.63 (m, 64H, aromatic), 3.69 (s, 48H, -OCH₃).

[*cis*-Mo₂(DAniF)₂]₄(O₂CFCO₂)₄ (**3**, Fc = Ferrocene). Crude product was recrystallized from CH₂Cl₂/hexanes solution. The product was yellow. Yield: 234 mg, 80%. Anal. Calcd (found) for **3**, C₁₆₈H₁₅₂-Fe₄Mo₈N₁₆O₃₂: C, 51.76 (51.33); H, 3.93 (3.92); N, 5.75 (5.68). Single crystals suitable for X-ray analysis were grown by diffusion of hexanes into a CH₂Cl₂ solution. ¹H NMR δ (ppm, in CD₂Cl₂): 8.68 (s, 8H, -NCHN-), 6.69 (m, 64H, aromatic), 5.05 (d, 16H, Cp ring), 4.16 (t, 16H, Cp ring), 3.69 (s, 48H, -OCH₃).

[*cis*-Mo₂(DAniF)₂]₄(O₂CC₆H₄C₆H₄CO₂)₄ (**4**). Crude product was recrystallized from CH₂Cl₂/EtOH solution. The product was red. Yield: 281 mg, 98%. Anal. Calcd (found) for **4**·2EtOH, C₁₈₀H₁₆₄-Mo₈N₁₆O₃₂: C, 55.96 (55.84); H, 4.28 (4.29); N, 5.80 (5.78). Single crystals suitable for X-ray analysis were grown by diffusion of CH₃CN into a CH₂Cl₂ solution. ¹H NMR δ (ppm, in CD₂Cl₂): 8.47 (d, 16H, -O₂CC₆H₄C₆H₄CO₂-), 8.36 (s, 8H, -NCHN-), 7.77 (d, 16H, -O₂CC₆H₄C₆H₄CO₂-), 6.67 (m, 64H, aromatic), 3.70 (s, 48H, -OCH₃).

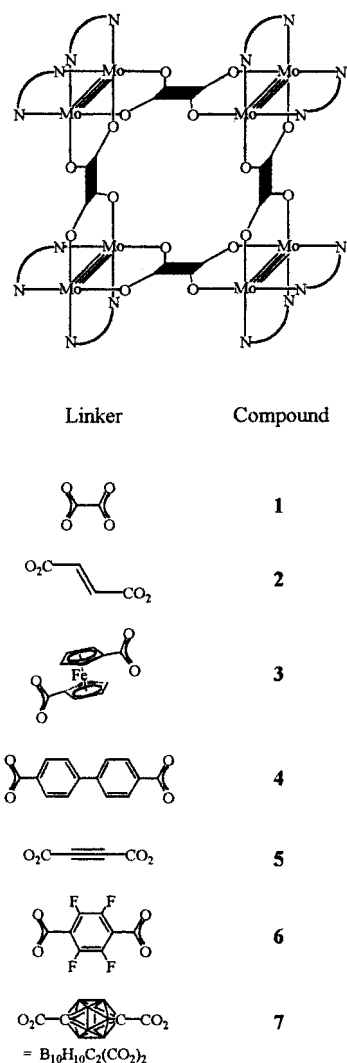
[*cis*-Mo₂(DAniF)₂]₄(O₂CC≡CCO₂)₄ (**5**). Crude product was recrystallized from CH₂Cl₂/CH₃OH solution. The product was red. Yield: 199 mg, 78%. Anal. Calcd (found) for **5**·CH₂Cl₂·2CH₃OH, C₁₃₉H₁₃₀-Cl₂Mo₈N₁₆O₃₄: C, 49.00 (48.37); H, 3.85 (3.83); N, 6.58 (6.45). ¹H NMR δ (ppm, in CD₂Cl₂): 8.51 (s, 8H, -NCHN-), 6.66 (m, 64H, aromatic), 3.69 (s, 48H, -OCH₃).

[*cis*-Mo₂(DAniF)₂]₄(O₂CC₆F₄CO₂)₄ (**6**). Crude product was recrystallized from CH₂Cl₂/hexanes solution. The product was dark-red. Yield: 239 mg, 85%. Anal. Calcd (found) for **6**, C₁₅₂H₁₂₀F₁₆-Mo₈N₁₆O₃₂: C, 48.63 (47.60); H, 3.22 (3.39); N, 5.97 (5.98). ¹H NMR δ (ppm, in CD₂Cl₂): 8.57 (s, 8H, -NCHN-), 6.71 (m, 64H, aromatic), 3.71 (s, 48H, -OCH₃).

[*cis*-Mo₂(DAniF)₂]₄(O₂CCB₁₀H₁₀CCO₂)₄ (**7**). Crude product was recrystallized from CH₂Cl₂/hexanes solution. The product was yellow. Yield: 278 mg, 92%. Anal. Calcd (found) for **7**·3CH₂Cl₂·0.5(hexane), C₁₄₂H₁₇₃B₁₀Cl₆Mo₈N₁₆O₃₂: C, 42.33 (42.07); H, 4.33 (4.31); N, 5.56 (5.44). ¹H NMR δ (ppm, in CD₂Cl₂): 8.33 (s, 8H, -NCHN-), 6.62 (m, 64H, aromatic), 3.70 (s, 48H, -OCH₃).

Crystallographic Procedures. Single crystals suitable for X-ray analysis for all compounds were grown by diffusion of hexanes, toluene, or CH₃CN into a CH₂Cl₂ solution as described above. Single-crystal X-ray work on compounds **1–3** described here was performed on a

Scheme 3



Nonius FAST diffractometer utilizing the program MADNES.⁷ In each case a suitable crystal was mounted on the tip of a quartz fiber with a small amount of silicone grease or epoxy cement and transferred to a goniometer head. Cell parameters were obtained from an autoindexing routine and were refined with 250 reflections within a 2θ range of 18.1–41.6°. Cell dimensions and Laue symmetry for all crystals were confirmed with axial photographs. All data were corrected for Lorentz and polarization effects. Data were processed using an ellipsoid-mask algorithm (program PROCOR),⁸ and the program SORTAV⁹ was used to correct for absorption.

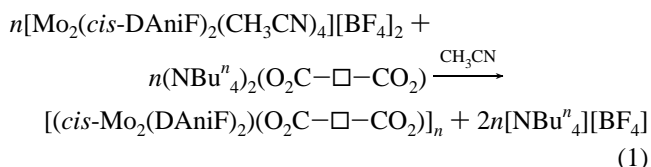
The data for **4** were collected on a Bruker SMART 2000 CCD detector system. Cell parameters were measured using the SMART¹⁰ software. Data were corrected for Lorentz and polarization effects using the program SAINT.¹¹ Absorption corrections were applied using SADABS.¹² Typically, crystals of **4** diffracted poorly. This is likely

due to the loss of solvent located in the large intermolecular cavity (vide infra). This is a common occurrence in supramolecular chemistry that often gives rise to high residuals in the least-squares refinement (e.g., $wR2$ of 0.20–0.30 or above).¹³ All other data collection procedures were similar to those used on the FAST diffractometer (vide supra).

In all structures, the positions of some or all of the non-hydrogen atoms were found via direct methods by way of the program package SHELXTL.¹⁴ For all structures, subsequent cycles of least-squares refinement followed by difference Fourier syntheses revealed the positions of the remaining non-hydrogen atoms. All hydrogen atoms were used in calculated positions. Other details of data collection and refinement for all complexes are given in Table 1. Selected atomic distances and angles are provided in Table 2. Other crystallographic data are available as Supporting Information.

Results and Discussion

Syntheses. In each case, reaction of $[\text{Mo}_2(\text{cis-DAniF})_2(\text{CH}_3\text{CN})_4][\text{BF}_4]_2$ with 1 equiv of the corresponding dicarboxylate anion in CH_3CN led to rapid formation of a precipitate and the subsequent isolation of a yellow to red product¹⁵ with a ratio of dimetal units, $\text{Mo}_2(\text{DAniF})_2$, to dicarboxylate of 1:1 in high yield. The purity was attested by ¹H NMR spectra and elemental analyses. Compounds **1–6** are moderately soluble in a few organic solvents such as CH_2Cl_2 , benzene, and toluene, but **7** is significantly less soluble. As shown in the reaction



with the predefined paddlewheel geometry of the Mo_2 group, a “square” with four Mo_2 units at the corners would be expected to form for $n = 4$. However, it should be noted that the triangles ($n = 3$) or loops ($n = 2$) shown in Scheme 2 would also have the same stoichiometry and that both are known to form in other cases.³ A structural characterization that followed for compounds **1–4** confirmed our expectation in those cases. Each crystal contains a large number of interstitial solvent molecules, and formation of crystals suitable for X-ray structural studies is very dependent on the solvents used. Numerous attempts to obtain suitable single crystals for the other three complexes have so far proved to be unrewarding. While we found that blocked-shaped crystals of **5** and **6** are obtainable, they are so fragile that gently touching them produces cracks that render them unsuitable for single-crystal X-ray analysis. Likewise, the tiny microcrystals of **7** that we have been able to grow from very dilute solutions do not diffract enough to obtain a suitable data set.

Structural Results. Thermal ellipsoid plots of compounds **1–4** are presented in Figure 1. Compound **1** crystallizes in the

(7) Pflugrath, J.; Messerschmitt, A. MADNES, Munich Area Detector (New EEC) System, version EEC 11/1/89, with enhancements by Nonius Corporation, Delft, The Netherlands. A description of MADNES appears in the following. Messerschmitt, A.; Pflugrath, J. *J. Appl. Crystallogr.* **1987**, *20*, 306.
 (8) (a) Kabsch, W. *J. Appl. Crystallogr.* **1988**, *21*, 67. (b) Kabsch, W. *J. Appl. Crystallogr.* **1988**, *21*, 916.
 (9) Blessing, R. H. *Acta Crystallogr.* **1995**, *A51*, 33.
 (10) SMART, Software for the CCD Detector System, version 5.5; Bruker Analytical Instruments Division: Madison, WI, 1998.
 (11) SAINT, Software for the CCD Detector System, version 5.06; Bruker Analytical Instruments Division: Madison, WI, 1997.
 (12) SADABS. Program for absorption correction using the Bruker CCD based on Blessing's method (see ref 9).

(13) (a) Iengo, E.; Milani, B.; Zangrando, E.; Geremia, S.; Alessio, E. *Angew. Chem., Int. Ed.* **2000**, *39*, 1096. (b) Mann, S.; Huttner, G.; Zsolnai, L.; Heinze, K. *Angew. Chem., Int. Ed. Engl.* **1996**, *35*, 2808. (c) Fujita, M.; Sasaki, O.; Mitsuhashi, T.; Fujita, T.; Yazaki, J.; Yamaguchi, K.; Ogura, K. *Chem. Commun.* **1996**, 1535. (d) Berseth, P. A.; Sokol, J. J.; Shores, M. P.; Heinrich, J. L.; Long, J. R. *J. Am. Chem. Soc.* **2000**, *122*, 9655. (e) Whang, D.; Park, K.-M.; Heo, J.; Ashton, P.; Kim, K. *J. Am. Chem. Soc.* **1998**, *120*, 4899. (f) Whang, D.; Kim, K. *J. Am. Chem. Soc.* **1997**, *119*, 451.
 (14) SHELXTL, version 5.03; Siemens Industrial Automation, Inc.: Madison, WI.
 (15) Of the seven compounds, those with ferrocene and borane linkers, **3** and **7**, are yellow. All others are red. We are presently carrying out a spectroscopic study of these and other compounds, which will be reported elsewhere.

Table 1. Crystal and Structure Refinement Data for Compounds **1–4**

	1 ·11CH ₂ Cl ₂	2 ·4.5(toluene)·1.4CH ₂ Cl ₂	3 ·2C ₆ H ₁₄	4 ·CH ₂ CN·0.1CH ₂ Cl ₂
chemical formula	C ₁₃₉ H ₁₄₂ Cl ₂₂ Mo ₈ N ₁₆ O ₃₂	C _{168.9} H _{166.8} Cl _{2.8} Mo ₈ N ₁₆ O ₃₂	C ₁₈₀ H ₁₈₀ Fe ₄ Mo ₈ N ₁₆ O ₃₂	C _{177.1} H _{153.7} Cl _{0.2} Mo ₈ N _{16.5} O ₃₂
fw	4096.11	3799.56	4070.32	3799.68
space group	<i>P</i> 2 ₁ / <i>n</i>	<i>P</i> $\bar{1}$	<i>P</i> $\bar{1}$	<i>P</i> $\bar{1}$
<i>a</i> , Å	19.089(1)	16.922(1)	16.951(3)	12.394(1)
<i>b</i> , Å	18.708(1)	17.570(6)	17.07(1)	28.572(2)
<i>c</i> , Å	23.708(1)	18.129(8)	20.935(8)	30.336(3)
α , deg		62.78(1)	103.84(2)	61.91(1)
β , deg	90.70(1)	73.09(2)	104.85(4)	81.46(2)
γ , deg		77.68(2)	105.92(3)	84.45(2)
<i>V</i> , Å ³	8465.9(7)	4565(3)	5309(4)	9368(1)
<i>Z</i>	2	1	1	2
temp, K	213(2)	273(2)	273(2)	213(2)
λ , Å	0.710 73	0.710 73	0.710 73	0.710 73
ρ_{calcd} , g cm ⁻³	1.607	1.382	1.273	1.347
μ , mm ⁻¹	0.991	0.642	0.782	0.590
R1, ^a wR2 ^b [<i>I</i> > 2 σ (<i>I</i>)]	0.075, 0.172	0.065, 0.166	0.085, 0.206	0.127, 0.221

^a R1 = $[\sum w(F_o - F_c)^2 / \sum wF_o^2]^{1/2}$. ^b wR2 = $[\sum [w(F_o^2 - F_c^2)^2] / \sum w(F_o^2)^2]^{1/2}$, $w = 1/[\sigma^2(F_o^2) + (aP)^2 + bP]$, where $P = [\max(F_o^2, 0) + 2(F_c^2)]/3$.

Table 2. Selected Bond Distances (Å) for Compounds **1–4**

Compound 1			
Mo(1)–Mo(2)	2.0865(8)	Mo(3)–Mo(4)	2.0940(8)
Mo(1)–N(1)	2.114(5)	Mo(3)–N(5)	2.101(5)
Mo(1)–N(3)	2.117(5)	Mo(3)–O(15)	2.112(4)
Mo(1)–O(9)	2.127(4)	Mo(3)–N(7)	2.116(5)
Mo(1)–O(11)	2.145(4)	Mo(3)–O(13)	2.144(4)
Mo(2)–N(2)	2.114(5)	Mo(4)–N(6)	2.098(5)
Mo(2)–O(12)	2.121(4)	Mo(4)–N(8)	2.111(5)
Mo(2)–N(4)	2.121(6)	Mo(4)–O(14)	2.119(4)
Mo(2)–O(10)	2.128(4)	Mo(4)–O(16)	2.139(4)
Compound 2			
Mo(1)–Mo(2)	2.087(1)	Mo(3)–Mo(4)	2.089(1)
Mo(1)–O(102)	2.115(5)	Mo(3)–O(103)	2.113(5)
Mo(1)–N(3)	2.120(6)	Mo(3)–N(5)	2.122(6)
Mo(1)–N(1)	2.127(6)	Mo(3)–N(7)	2.135(6)
Mo(1)–O(106)	2.127(5)	Mo(3)–O(107)	2.154(5)
Mo(2)–N(2)	2.111(6)	Mo(4)–N(8)	2.092(6)
Mo(2)–O(105)	2.114(5)	Mo(4)–O(108)	2.107(5)
Mo(2)–O(101)	2.133(5)	Mo(4)–N(6)	2.119(6)
Mo(2)–N(4)	2.136(6)	Mo(4)–O(104)	2.130(5)
Compound 3			
Mo(1)–Mo(2)	2.084(2)	Mo(3)–Mo(4)	2.075(2)
Mo(1)–N(1)	2.102(8)	Mo(3)–N(5)	2.119(8)
Mo(1)–N(3)	2.115(9)	Mo(3)–O(13)	2.125(7)
Mo(1)–O(9)	2.123(6)	Mo(3)–O(15)	2.138(7)
Mo(1)–O(11)	2.130(7)	Mo(3)–N(7)	2.140(8)
Mo(2)–N(2)	2.134(8)	Mo(4)–N(6)	2.089(8)
Mo(2)–N(4)	2.134(9)	Mo(4)–O(14)	2.122(7)
Mo(2)–O(10)	2.138(7)	Mo(4)–N(8)	2.138(8)
Mo(2)–O(12)	2.147(7)	Mo(4)–O(16)	2.140(7)
Compound 4			
Mo(1)–Mo(2)	2.089(4)	Mo(5)–Mo(6)	2.082(3)
Mo(1)–O(503)	2.121(14)	Mo(5)–N(9)	2.121(15)
Mo(1)–N(1)	2.149(17)	Mo(5)–O(509)	2.136(14)
Mo(1)–N(3)	2.152(18)	Mo(5)–O(511)	2.163(14)
Mo(1)–O(501)	2.159(13)	Mo(5)–N(11)	2.180(17)
Mo(2)–N(4)	2.106(17)	Mo(6)–N(10)	2.121(16)
Mo(2)–O(504)	2.136(14)	Mo(6)–O(512)	2.123(15)
Mo(2)–O(502)	2.139(13)	Mo(6)–N(12)	2.128(17)
Mo(2)–N(2)	2.167(17)	Mo(6)–O(510)	2.163(14)
Mo(3)–Mo(4)	2.075(4)	Mo(7)–Mo(8)	2.082(4)
Mo(3)–O(505)	2.123(15)	Mo(7)–O(515)	2.121(16)
Mo(3)–N(5)	2.131(19)	Mo(7)–N(15)	2.123(19)
Mo(3)–N(7)	2.138(16)	Mo(7)–O(513)	2.150(14)
Mo(3)–O(507)	2.157(13)	Mo(7)–N(13)	2.16(2)
Mo(4)–N(6)	2.086(18)	Mo(8)–O(514)	2.105(14)
Mo(4)–O(506)	2.121(15)	Mo(8)–N(14)	2.15(2)
Mo(4)–N(8)	2.138(17)	Mo(8)–N(16)	2.15(2)
Mo(4)–O(508)	2.154(13)	Mo(8)–O(516)	2.188(16)

monoclinic space group *P*2₁/*n* with an inversion center located at the center of the molecule. Each dimolybdenum unit consists

of an eclipsed paddlewheel arrangement, with two cis formamidate paddles; the other two are the oxalate linkers. Four such Mo₂ units are assembled into a square through the oxalate linkages. Two crystallographically independent quadruply bonded Mo–Mo distances are 2.0865(8) and 2.0940(8) Å. A disordered CH₂Cl₂ molecule is located at the center of the square, while 10 other CH₂Cl₂ molecules fill other interstices in the unit cell. Except for the absence of axial ligands on the metal–metal bonded unit, this structure resembles that of the rhodium analogue also reported in our preliminary communication.³ The square arrangement of **1** is also reminiscent of another rhodium complex containing benzene-1,4-dicarboxylate anions as linkers.¹⁶

Compounds **2–4** crystallize in the triclinic space group *P* $\bar{1}$. As in **1**, there is again a crystallographic inversion center located at the midpoint of each molecule. The crystallographically independent Mo–Mo distances are 2.087(1), 2.089(1) Å for **2**, 2.084(2), 2.075(2) Å for **3**, and 2.089(4), 2.075(4), 2.082(3), 2.082(4) Å for the two crystallographically independent molecules in **4**; these are typical quadruply bonded Mo₂ distances. Other bond distances and bond angles for all compounds are similar to those found in other dimolybdenum paddlewheel complexes.

The crystal packing of these compounds shows very interesting features. For **1** and **2**, the squares formed by the midpoints of the four Mo–Mo axes stack directly on top of each other creating a square channel, as shown in the right side of Figure 1. For **3**, the 1,1'-ferrocenium dicarboxylate groups adopt an anti configuration in order to form a square of Mo₂ units. These molecules also stack directly on top of each other, but now the channels have a more complex shape. Molecules of **4** are again stacked, but alternate square layers are staggered by ca. 45° so that the squares of every other layer are superposed, giving a channel with an octagonal shape. Thus, by changing the size and shape of the linker, one can vary not only the size and shape of the oligomers but also the size and shape of the channels within the crystal. The area of the square formed by the core of each molecule is estimated to be ca. 7 × 7, 9 × 9, 10 × 10, and 15 × 15 Å² for **1**, **2**, **3**, and **4**, respectively. All structurally characterized compounds have solvent molecules in intermolecular interstices of the crystal and also within the square channels. Furthermore, each shows a preference for a particular solvent. Dichloromethane is found in **1**, toluene in **2**, disordered partially occupied hexanes in **3**, and partially occupied dichlo-

(16) Bonar-Law, R. P.; McGrath, T. D.; Singh, N.; Bickley, J. F.; Steiner, A. *Chem. Commun.* **1999**, 2457.

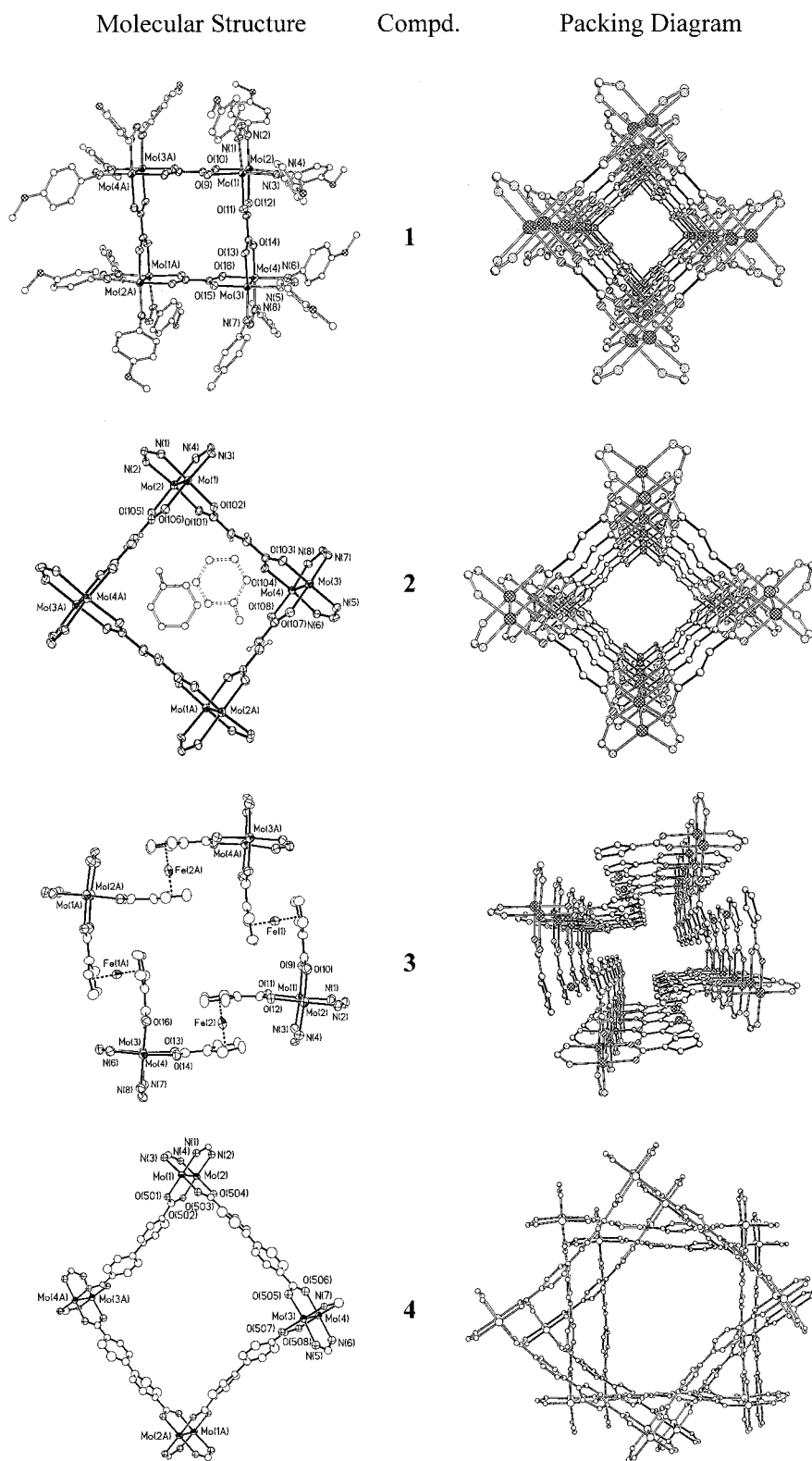


Figure 1. Cores (on the left) and packing diagrams (on the right) for the molecular squares **1–4**. For simplicity, hydrogen atoms and the *p*-anisyl groups on each N atom (except for **1**) have been removed. For the cores, atoms are drawn at the 40% probability level. Except for **2**, interstitial solvent molecules are not shown.

romethane and acetonitrile in **4**. These can also be observed in the NMR spectra. In each case, no other solvent has provided good single crystals. This might be an indication that size selectivity could be an important property of these channels. However, this remains to be further investigated.

Solution Behavior. Before discussing the data per se, the question of what species are present in solution must be

addressed. For any compound consisting of $\text{Mo}_2(\text{DAniF})_2$ corner units and dicarboxylate linkers, O_2CXCO_2 , in a 1:1 ratio, there are no less than three possible structures: loops of molecular formula $[\text{Mo}_2(\text{DAniF})_2(\text{O}_2\text{CXCO}_2)]_2$, triangles, $[\text{Mo}_2(\text{DAniF})_2(\text{O}_2\text{CXCO}_2)]_3$, and squares, $[\text{Mo}_2(\text{DAniF})_2(\text{O}_2\text{CXCO}_2)]_4$. It seems clear that loops¹⁷ can form only when the linkers are either permanently bent (e.g., malonate) or can easily become bent

(e.g., 1,4-phenylenediacetate). Otherwise the strain would be far too great. However, the question of triangles vs squares, even with linkers that prefer to be linear, is not so simple. While it might seem "obvious" that for an assembly of corners that strongly favor a 90° angle between linkers and linkers that favor linearity, the formation of squares is the "only logical result", and we already have two examples where the "obvious" is not correct.

In the case of $[\text{Rh}_2(\text{DAniF})_2(\text{O}_2\text{CCO}_2)_n]$, we have actually found that the species with $n = 3$ is about as stable as that with $n = 4$. One factor that contributes to this surprising result is that the Rh_2^{4+} unit has no inherent resistance to twisting about the Rh–Rh axis because there is only a net σ bond in this species that has a $\sigma^2\pi^4\delta^2\delta^*2\pi^{*4}$ configuration. Thus, some of the potential strain in the three-membered ring is relieved in that way. While the Mo_2^{4+} unit is rotationally more rigid because it has a net δ bond, it would not be expected to readily form a triangle with such a rigid linker as the oxalate ion, and there is no evidence that it does. However, we have found that with the linker *trans*-1,4-cyclohexanedicarboxylate and the corner piece $\text{Mo}_2(\text{DAniF})_2$, a triangle is formed, and it has been structurally characterized in the crystalline state.¹⁸

The point of all these prefatory remarks is to make it clear that one must be at least a little circumspect in interpreting the solution data for the seven presumably square compounds reported here. Compounds 1–4 have been shown to be square in the crystalline state, but there is no guarantee that a transformation to triangles in solution does not occur. As for compounds 5–7, we have been unable to obtain useful single crystals so that even as solids we are not certain that they are squares.

For each of the seven compounds, the ¹H NMR spectrum showed one signal for the methine protons, one for the CH₃ groups, and only a single multiplet for the aromatic hydrogen atoms. This implies a highly symmetric structure such as a triangle or a square but does not tell us which. It cannot even be used to rule out a mixture in solution, as shown by the case of the $[\text{Rh}_2(\text{DAniF})_2(\text{O}_2\text{CCO}_2)]_{3/4}$ mixture, where there was no doubling of the ¹H signals despite the presence of both species in comparable amounts.

All of these cautionary remarks notwithstanding, we believe it is reasonable to presume that each of these seven compounds does consist entirely of square molecules in solution. As we shall now see, there is nothing in the electrochemical results to suggest otherwise.

Electrochemistry. It is well-known that in all dimolybdenum formamidinate compounds the Mo_2^{4+} unit can undergo a one-electron oxidation process. We have observed that oxidation processes are also possible in systems where dimetal units are coupled by dicarboxylate linkers. The study of electronic coupling between such Mo_2^{4+} units is an important priority for us.

The electrochemical results for the seven squares are displayed in Figure 2 and presented numerically in Table 3. Our purpose in making these measurements is to find what levels of oxidation are available to the various squares. This will depend, in considerable measure, on how the various dicarboxylate linkers will establish communication¹⁹ between the individual dimolybdenum units. This has already been assessed

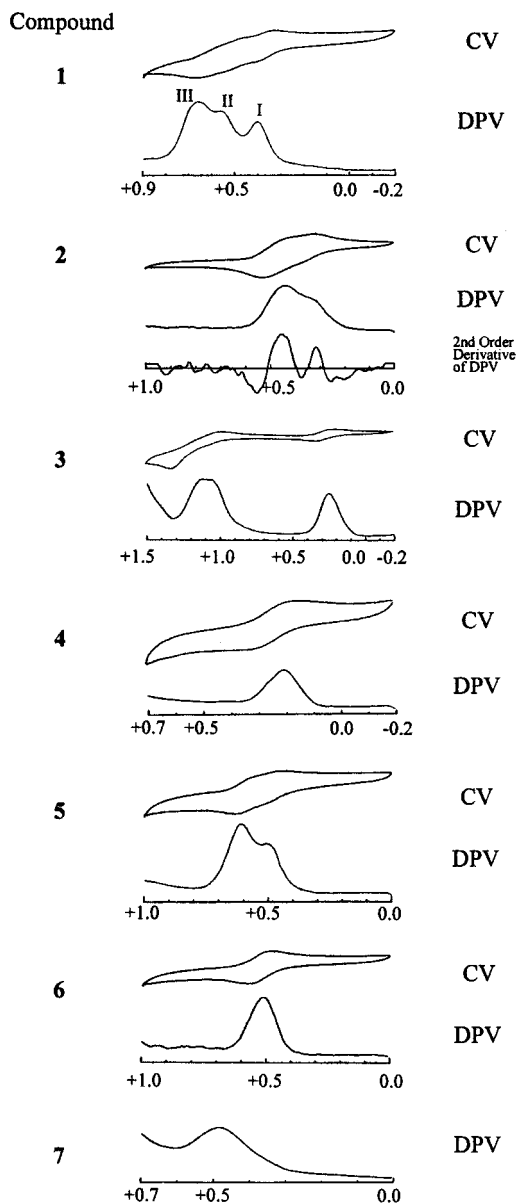


Figure 2. Cyclic and differential pulse voltammograms for compounds 1–6. Only the latter is shown for the irreversible oxidation of 7.

for the simpler $[\text{Mo}_2]\text{O}_2\text{C}-\text{X}-\text{CO}_2[\text{Mo}_2]$ compounds with the same linkers, X, that are found in compounds 1–3 and 5–7 of the present study. We now ask whether the results for squares 1–3 and 5–7 are consistent with those previously obtained in the corresponding $[\text{Mo}_2]\text{O}_2\text{C}-\text{X}-\text{CO}_2[\text{Mo}_2]$ compounds.²⁰ The first thing to look at is how much the first oxidation potential is shifted in going from the simpler compound to the square with the same linker. These comparisons are tabulated in Table 4. As expected, in every case there is a shift to a more positive potential because replacement of formamidinate ligands by carboxylate ligands destabilizes the oxidized species. However, the magnitudes of the shifts vary from +82 to +208 mV, although for 1–3 and 5–7 the range is only 146–208 mV. This variation is probably related to the varying basicities of the carboxylate anions, but this is impossible to establish quantitatively because data on the strengths of the various acids is not generally available. The peculiarly low value in the case of ferrocene dicarboxylate bridges has no obvious explanation.

(17) Cotton, F. A.; Lin, C.; Murillo, C. A. *Inorg. Chem.* **2001**, *40*, 472.

(18) Cotton, F. A.; Lin, C.; Murillo, C. A. *Inorg. Chem.* **2001**, *40*, 575.

(19) Dicarboxylate anions bridging mononuclear species have been used to study possible intermolecular interactions. Clauss, A. W.; Wilson, S. R.; Buchanan, R. M.; Pierpont, C. G.; Hendrickson, D. N. *Inorg. Chem.* **1983**, *22*, 628.

(20) Cotton, F. A.; Donahue, J. P.; Lin, C.; Murillo, C. A. *Inorg. Chem.*, accepted.

Table 3. Redox Potentials,^a $E_{1/2}$ in mV,^b for the Oxidation Processes Accessible to Compounds 1–7

Compd.	Redox Potentials		
1	$-e \rightarrow$ 407	$-e \rightarrow$ 567	$-e \rightarrow$ 661
2	$-e \rightarrow$ 363	$-2e \rightarrow$ 453	
3	$-3e \rightarrow$ 274		
4	$-3e \rightarrow$ 233		
5	$-e \rightarrow$ 518	$-2e \rightarrow$ 621	
6	$-3e \rightarrow$ 523		
7	$-3e \rightarrow$ 497		

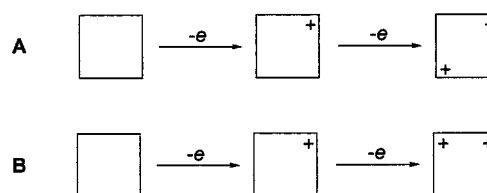
^a The electrochemical data were recorded on a BAS 100 electrochemical analyzer in 0.10 M Buⁿ₄NPF₆ solution (CH₂Cl₂) with Pt working and auxiliary electrodes and a Ag/AgCl reference electrode. Scan rate was 100 mV s⁻¹ for CV and 2 mV s⁻¹ for DPV. All potential values are referenced to the Ag/AgCl, and under the present experimental conditions, the $E_{1/2}(\text{Fc}^+/\text{Fc})$ was consistently measured to be 440 mV. ^b $E_{1/2} = E_p + E_{\text{pul}}/2$ and $E_{\text{pul}} = 25$ mV from DPV.

Table 4. Comparison of Oxidation Potentials (mV) of Presumably Square Compounds with That of the Linear [(DAniF)₃Mo₂]₂(O₂C–□–CO₂) Compounds

compd	bridge	potential of 1st oxidation			separation of 1st and 2nd oxidations	
		linear	square	difference	linear	square
1	–O ₂ CCO ₂ –	260	407	147	212	160
2	–O ₂ CCHCHCO ₂ –	217	363	146	117	90
3	–O ₂ CFcCO ₂ –	192	274	82	0	0
5	–O ₂ CCCCO ₂ –	325	518	193	108	103
6	–O ₂ CC ₆ F ₄ CO ₂ –	315	523	208	41	0
7	–O ₂ CCB ₁₀ H ₁₀ CCO ₂ –	328	497	169	0	0

We next compare the differences between the first and second oxidation potentials for the linear compounds and the squares. This is done in terms of the peak-to-peak separations in the differential pulse voltammetry (DPV) results, and the results are also listed in Table 4. The two lists are in moderately good agreement with each other, but there is a significant discrepancy for the oxalates for which we can suggest only one explanation. The second oxidation in the square must be occurring at the dimolybdenum unit diagonally across from the first one rather than adjacent to it (case A, Scheme 4). This naturally means that the first oxidation has a weaker influence than it would on the adjacent sites.

For the linear compounds corresponding to the present compounds 3, 6, and 7 the coupling of the two dimolybdenum units was very weak (in two cases, resolved DPV peaks were not seen), and therefore, it is entirely to be expected that resolved

Scheme 4

peaks are not seen here. For compounds 2 and 5, however, the agreement with the results for the corresponding linear species is not the expected result and is not easy to explain. As in the case of 1, we might expect that the second oxidation would occur at the remote corner and therefore, as in the case of 1, at a voltage closer to that of the first oxidation than for the corresponding linear species. The actual results would seem to suggest that, instead of case A in Scheme 4, we have case B. But if this is true, why is it so in these compounds but not in compound 1? That is a question we cannot at present answer should the structure in solution be that of a square.

A few other remarks concerning the electrochemistry of the square compound are necessary. In compound 3, the irreversible oxidation observed at E_{pa} of 1330 mV occurs in the ferrocene group or groups. To determine the number of electrons involved in the oxidation steps for each compound, either Mo₂[(*p*-CH₃C₆H₄N)₂CH]₄ or Mo₂[(*m*-CF₃C₆H₄N)₂CH]₄ was added as internal standards. (These two paddlewheel-type compounds undergo only one-electron oxidations.)²¹ For each compound, three DPV experiments were done by varying the Mo₂/(Mo₂)₄ ratios, these being 1:1, 2:1, and 3:1. A careful determination of the areas under each DPV peak reveals that the total number of electrons involved in the oxidations of dimolybdenum centers for compounds 1–7 is only three. Thus, compound 3 could have a maximum of charge of +7 (three molybdenum-based oxidation processes and up to four ferrocene-based oxidations).

Acknowledgment. We are grateful to the National Science Foundation for support of the work, to Dr. Lee M. Daniels for helpful crystallographic advice, and to Prof. S. B. Kahl of the Department of Pharmaceutical Chemistry, University of California, San Francisco for supplying the B₁₀H₁₀C₂(CO₂H)₂.

Supporting Information Available: An X-ray crystallographic file for compounds 1–4, in CIF format. This material is available free of charge via the Internet at <http://pubs.acs.org>.

IC001016T

(21) Lin, C.; Protasiewicz, J. D.; Smith, E. T.; Ren, T. *Inorg. Chem.* **1996**, *35*, 6422.